

## Classification of Strange Attractors by Integers

Gabriel B. Mindlin,<sup>(1)</sup> Xin-Jun Hou,<sup>(1)</sup> Hernán G. Solari,<sup>(1)</sup> R. Gilmore,<sup>(1)</sup> and N. B. Tufillaro<sup>(2)</sup>

<sup>(1)</sup>*Department of Physics and Atmospheric Science, Drexel University, Philadelphia, Pennsylvania 19104-9984*

<sup>(2)</sup>*Department of Physics, Bryn Mawr College, Bryn Mawr, Pennsylvania 19010-2899*

(Received 4 December 1989)

We show how to characterize a strange attractor by a set of integers. These are extracted from the chaotic time-series data by first reconstructing the low-period orbits and then determining the template, or knot holder, which supports all periodic orbits embedded in the strange attractor, and the strange attractor itself. The template is identified by a set of integers which therefore characterize the strange attractor. This identification is explicitly demonstrated for the Pirogon using a relatively small data set (5000 points).

PACS numbers: 05.45.+b

Two general approaches have been applied to the description of strange attractors. The metric approach<sup>1-8</sup> depends on dynamical information and the topological approach<sup>9-11</sup> is based on the properties of periodic orbits which are embedded in the strange attractor. Metric properties provide information about expansion rates and local structure of the strange attractor which remains invariant under coordinate-system changes but which depends on control parameters. Topological indices provide information about the organization of the strange attractor which is independent of coordinate-system changes and which also remains invariant under control-parameter variation.

In the first approach, time-series data are used to compute metric invariants such as fractal dimension,<sup>1</sup> metric entropy,<sup>2</sup> the Lyapunov exponent,<sup>3-5</sup> and the spectrum of singularities,  $f(\alpha)$ .<sup>6</sup> These are averaged quantities sampled over the entire strange attractor. They are difficult to compute and require large data sets. They return relatively little information for the amount of computational effort invested. For example, computation of fractal dimension is typically done by embedding the data in a sequence of spaces of increasing dimension, using a box-counting algorithm depending on some small distance  $\epsilon$ , and looking for stable limits as  $\epsilon$  decreases and the embedding dimension increases. Convergence is often problematic.<sup>12</sup> The result of the calculation is a real number with larger or smaller error bars that does not say much about "how to model the dynamics."<sup>10</sup>

In the topological approach<sup>9-11</sup> the goal is to determine how the unstable periodic orbits, which are embedded in the strange attractor, are intertwined.<sup>11</sup> Since periodic orbits are dense in a hyperbolic strange attractor,<sup>13</sup> knowledge of their linking properties severely constrains the topology of the strange attractor.

In the completely hyperbolic limit all periodic orbits are described by the symbolic dynamics on a complete  $n$ -ary tree. Flows in which a horseshoe (annulus) map is suspended have periodic orbits described by a complete binary (ternary) tree. As a control parameter is changed, the unstable periodic orbits are annihilated

("pruned"). The strange attractor is described by the spectrum and symbolic dynamics of the remaining periodic orbits and by their linking properties. The organization of the remaining orbits is not changed by the pruning process. In addition, there is evidence of topological universality in this pruning process.<sup>14</sup>

The organization of the unstable periodic orbits embedded in the strange attractor is described by their relative rotation rates and linking numbers.<sup>15,16</sup> The relative rotation rate of two periodic orbits is the average number of times one orbit rotates about the other per period. These topological indices are computed for all pairs of periodic orbits which can be reconstructed from the chaotic time-series data using the method of close returns.<sup>7-12</sup> This matrix of rational fractions is then compared with tables of relative rotation rates for strange attractors generated from known mechanisms (Smale horseshoe,<sup>17,18</sup> annulus map,<sup>19</sup> and Lorenz flow<sup>20,21</sup>). This serves to identify the topology of the strange attractor. There is, in addition, predictive capability. Once the mechanism responsible for creating the strange attractor has been identified, the relative rotation rates for all pairs of periodic orbits can be computed. These must agree with the relative rotation rates for any additional orbits extracted from the time-series data. If not, the identification is incorrect. Thus the topological classification of a strange attractor may be shown invalid, a feature notably absent from the metric characterization of strange attractors.

The computation of relative rotation rates proceeds algorithmically once the template,<sup>20,21</sup> or knot holder, which is responsible for the generation of a hyperbolic strange attractor, has been identified. A template is a branched surface which is particularly convenient for visualizing flows in a dynamical system. Templates for the Smale horseshoe, the Lorenz flow, the Pirogon, and the Smale horseshoe with a global torsion<sup>16</sup> of  $+1$  are shown in Fig. 1. It is useful to describe templates algebraically. Two pieces of information are required for this description. The first is an  $n \times n$  matrix, where  $n$  is the number of components of the template, or branches

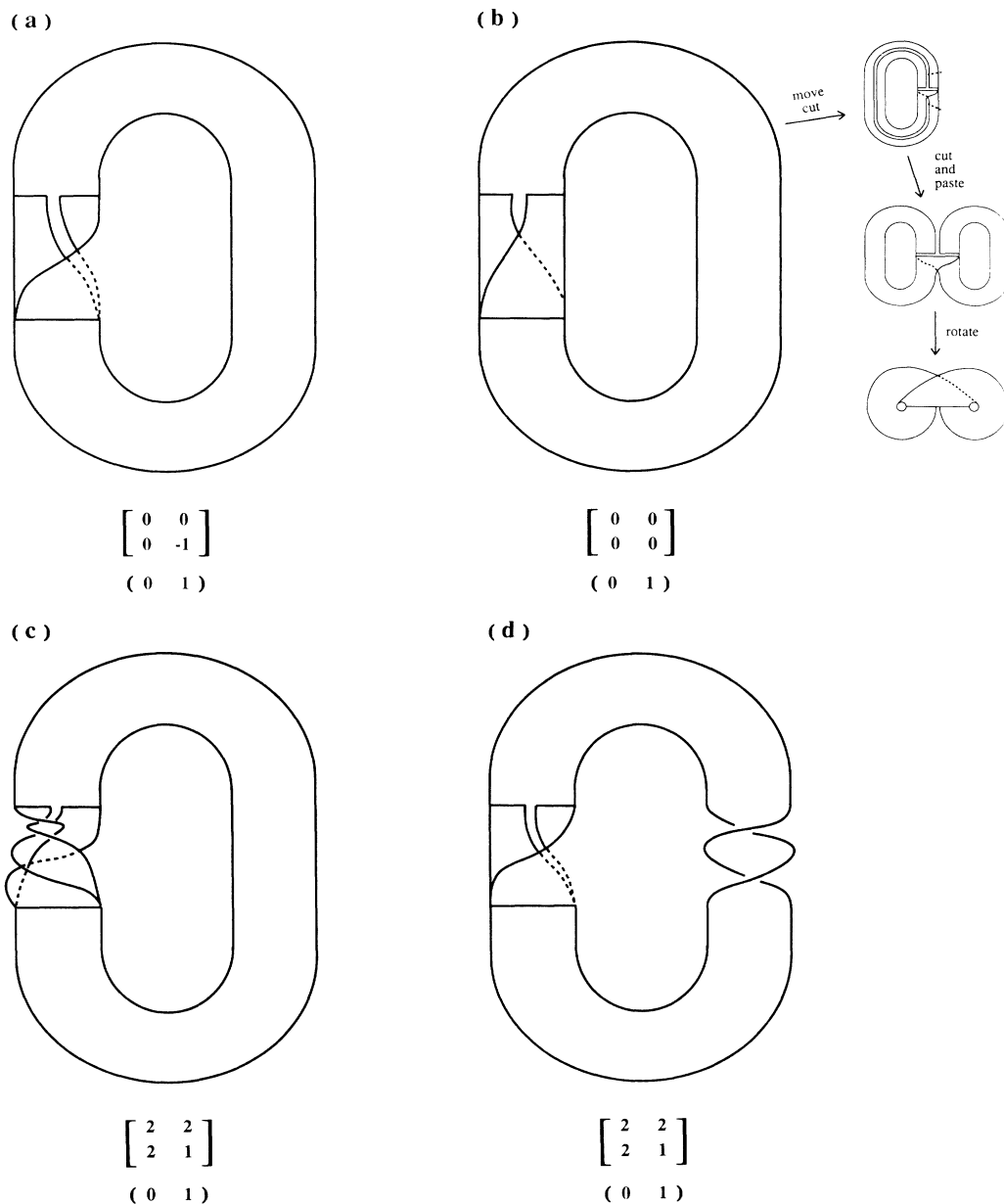


FIG. 1. Templates are shown for four flows. Beneath each template is its algebraic representation, consisting of the template matrix and the organization of the template components. (a) Smale horseshoe; (b) Lorenz flow, showing equivalence with the more familiar Lorenz mask; (c) Pirogon; and (d) Smale horseshoe with global torsion of +1. The flows (c) and (d) are topologically equivalent.

in the branched manifold. The second piece of information determines the order in which the branches are reconnected at the bottom of the template.

The diagonal elements of the template matrix describe the local torsion of the corresponding branch of the template, measured in units of  $\pi$ . An even (odd) matrix element indicates an orientation-preserving (-reversing) branch. The diagonal matrix elements also describe the local torsion of the single period-one orbit embedded in each branch. The off-diagonal elements of the template matrix are (twice) the linking numbers of the period-one

orbits embedded in the corresponding branches. A  $1 \times n$  array identifies the order (from back to front) in which the branches are glued together. The template matrix and layer-organization information are shown below the four templates in Fig. 1.

The relative rotation rates can be computed from the template matrix and layer-organization information. Conversely, the template matrix can be reconstructed from the relative rotation rates of the period-one orbits, and the layer organization can be determined from the relative rotation rates of some of the period-two orbits.

This suggests that the template itself can be reconstructed from the chaotic time-series data by extracting only the period-one and period-two orbits. The integers of the template matrix and the layer-organization information then characterize the topological structure of the strange attractor. Further, this identification can be confirmed or invalidated by pulling higher-period orbits out of the chaotic time-series data and comparing their relative rotation rates with those computed from the template.

We tested these ideas on a chaotic time series generated by the Pirogon,<sup>22</sup> one of the laboratories for testing topological ideas in nonlinear dynamics,

$$x'' + (4bx^2 - 2a)x' + bx^3(bx^2 - 2a) + (a^2 + \omega^2)x = \sum_{j=-\infty}^{\infty} V_E \delta(t - jT_E) \quad (1)$$

for  $a = \omega = b/10 = 1.57079$ ,  $V_E = \frac{13}{8}$ , and  $T_E = 2.61$ . A small sample of 5000 data points in the variables  $x$  and  $x' = dx/dt$  was collected. Orbits of low period were reconstructed from the time-series data.

Two period-one orbits and one period-two orbit were initially reconstructed. The strange attractor and the three reconstructed orbits are shown in Fig. 2. The linking number of the period-one orbits was computed ( $L = 1$ ) giving the off-diagonal elements of the template matrix. The local torsion for each period-one orbit was determined by computing how each pair of strange-attractor segments near the period-one orbit wound around each other. For one orbit all nearby segments linked once (regular saddle), for the other orbit all pairs linked  $\frac{1}{2}$  times (flip saddle). The corresponding diagonal matrix elements are 2 and 1. The period-two orbit was used to distinguish the two folding possibilities. The

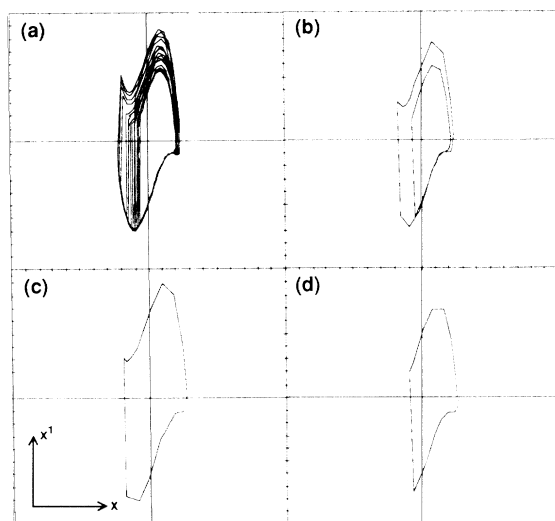


FIG. 2. (a) The strange attractor for the symmetrically kicked Pirogon [Eq. (1)] with (b) a period-two and (c), (d) two period-one orbits reconstructed from the chaotic time series.

one identified is compatible with continuity of the flow over the branched manifold.

To verify this identification we extracted some period-three and period-four orbits from the chaotic time-series data. Their relative rotation rates with respect to the previously reconstructed orbits and also to each other were then determined and compared with those predicted using the template matrix constructed above [Fig. 1(c)]. There were no discrepancies.

We should point out that the Pirogon template is identical to the template for the Smale horseshoe with a full twist (global torsion of +1). Thus, flows on the two templates are very similar—indistinguishable in the Poincaré section—but the strange attractors cannot be continuously deformed into each other.

As a second test of this procedure, we investigated the strange attractor generated by the antisymmetrically kicked Pirogon,<sup>23</sup>

$$x'' + (4bx^2 - 2a)x' + bx^3(bx^2 - 2a) + (a^2 + \omega^2)x = \sum_{j=-\infty}^{\infty} V_E (-1)^j \delta(t - jT_E/2) \quad (2)$$

for  $a = \omega = b/10 = 1.57079$ ,  $V_E = \frac{13}{8}$ , and  $T_E = 4.6535$ . We found four orbits of period one and six of period two. The template matrix and layer information constructed from these orbits are shown in Fig. 3. The template associated with this matrix and layer-organization information is also shown in Fig. 3. The correctness of this template and its algebraic representation was confirmed in three ways.

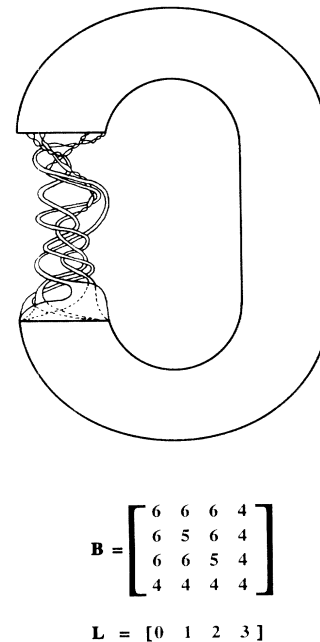


FIG. 3. Four-component template for the antisymmetrically kicked Pirogon [Eq. (2)] which is reconstructed from the chaotic time series and its algebraic representation.

(i) Higher-period orbits were extracted from the chaotic time-series data, their relative rotation rates were computed and compared with those determined using this template. There were no discrepancies.

(ii) The template  $P_A$  for the antisymmetrically kicked Pirogon is related to the template for the symmetrically kicked Pirogon  $P_S$  by  $P_A = (-I_0 P_S)^2$ , where  $I_0$  describes a single-component template with a half twist. The template  $(-I_0 P_S)^*(-I_0 P_S)$  was drawn by hand and is topologically equivalent to that shown in Fig. 3.

(iii) We constructed the template matrix for  $P_A$  by concatenating the template matrices  $P_S$  and  $I_0$  ( $-I_0^* P_S$ ), and then concatenating this template matrix with itself:  $(-I_0^* P_S)^*(-I_0^* P_S)$ .<sup>24</sup> The resulting template matrix and layer-organization information are identical to those extracted from the data.

We have described and tested a procedure for identifying the topology of a strange attractor. The identification is made in terms of a set of integers. These are the elements of the template matrix and the layer-organization information. The parity of the diagonal elements of this matrix define the return map; the remaining elements are properties of the flow. These integers can be extracted from the period-one and period-two orbits reconstructed from a relatively small data set, 5000 points in the present case. The template serves to model the qualitative dynamics of the system. The identification can be confirmed or invalidated by investigating orbits of higher period reconstructed from the time-series data.

We would like to thank N. B. Abraham and A. M. Albano, co-organizers of the International Workshop on Quantitative Measures of Dynamical Complexity in Nonlinear Systems, where some of the ideas presented here came into focus. One of the authors (G.B.M.) thanks M. O. Magnasco for useful discussions. Another one of the authors (H.G.S.) wishes to thank Consejo Nacional de Investigaciones Científicas y Técnicas (CONICET) of Argentina. This work was supported in part by NSF Grant No. PHY 88-43235.

<sup>1</sup>P. Grassberger and I. Procaccia, Phys. Rev. A **28**, 2591 (1983).

<sup>2</sup>I. Procaccia, Phys. Scr. **T9**, 40 (1985).

<sup>3</sup>A. Wolf, J. B. Swift, H. L. Swinney, and J. A. Vastano, Physica (Amsterdam) **16D**, 285 (1985).

<sup>4</sup>M. Sano and Y. Sawada, Phys. Rev. Lett. **55**, 1082 (1985).

<sup>5</sup>J.-P. Eckmann, S. O. Kamphorst, D. Ruelle, and S. Ciliberto, Phys. Rev. A **34**, 497 (1986).

<sup>6</sup>T. C. Halsey, M. H. Jensen, L. P. Kadanoff, I. Procaccia, and B. I. Shraiman, Phys. Rev. A **33**, 1141 (1986); **34**, 1601(E) (1986).

<sup>7</sup>C. Grebogi, E. Ott, and J. A. Yorke, Phys. Rev. A **36**, 3522 (1988).

<sup>8</sup>D. Auerbach, B. O'Shaughnessy, and I. Procaccia, Phys. Rev. A **37**, 2234 (1988).

<sup>9</sup>P. Cvitanović, G. H. Gunaratne, and I. Procaccia, Phys. Rev. A **38**, 1503 (1988).

<sup>10</sup>G. H. Gunaratne, P. S. Linsay, and M. J. Vinson, Phys. Rev. Lett. **63**, 1 (1989).

<sup>11</sup>N. B. Tufillaro, H. G. Solari, and R. Gilmore, Phys. Rev. A (to be published).

<sup>12</sup>D. P. Lathrop and E. J. Kostelich, Phys. Rev. A **40**, 4028 (1989).

<sup>13</sup>R. Devaney and Z. Nitecki, Commun. Math. Phys. **67**, 137 (1979).

<sup>14</sup>G. H. Gunaratne, M. H. Jensen, and I. Procaccia, Nonlinearity **1**, 157 (1988).

<sup>15</sup>H. G. Solari and R. Gilmore, Phys. Rev. A **37**, 3096 (1988).

<sup>16</sup>H. G. Solari and R. Gilmore, Phys. Rev. A **38**, 1566 (1988).

<sup>17</sup>S. Smale, Bull. Am. Math. Soc. **73**, 747 (1967).

<sup>18</sup>P. J. Holmes and R. F. Williams, Arch. Ration. Mech. Anal. **90**, 115 (1985).

<sup>19</sup>K. Hockett and P. J. Holmes, Ergodic Theory Dynamical Systems **6**, 205 (1986).

<sup>20</sup>R. F. Williams, Inst. Hautes Études Sci. Publ. Math. **50**, 73 (1979).

<sup>21</sup>J. S. Birman and R. F. Williams, Topology **22**, 47 (1983).

<sup>22</sup>D. L. Gonzalez and O. Piro, Phys. Rev. Lett. **50**, 870 (1983).

<sup>23</sup>D. L. Gonzalez and O. Piro, Phys. Rev. Lett. **55**, 17 (1985).

<sup>24</sup>R. Gilmore and G. B. Mindlin (unpublished).